Stabilizing the open conformation of the integrin headpiece with a glycan wedge increases affinity for ligand

Bing-Hao Luo*†, Timothy A. Springer*†, and Junichi Takagi*‡§

*Center for Blood Research and Departments of †Pathology and ‡Pediatrics, Harvard Medical School, Boston, MA 02115

Contributed by Timothy A. Springer, December 31, 2002

The affinity of the extracellular domain of integrins for ligand is regulated by conformational changes signaled from the cytoplasm. Alternative types of conformational movement in the ligand-binding headpiece have been proposed. In one study, electron micrograph image averages of the headpiece of integrin aVβ3 show two different conformations. The open conformation of the headpiece is present when a ligand mimetic peptide is bound and differs from the closed conformation in the presence of an obtuse angle between the β3 subunit hybrid and I-like domains. We tested the hypothesis that opening of the hybrid-I-like domain interface increases ligand-binding affinity by mutationally introducing an N-glycosylation site into it. Both β3 and β1 integrin glycan wedge mutants exhibit constitutively high affinity for physiological ligands. The data uniquely support one model of integrin activation and suggest that movement at the interface with the hybrid domain pulls down the C-terminal helix of the I-like domain and activates its metal ion-dependent adhesion site, analogously to activation of the integrin I domain.

Integrins are a family of ≈25 cell adhesion molecules that mediate cell–cell, cell–extracellular matrix, and cell–pathogen interactions and govern migration and anchorage of almost all kinds of cells. Integrins are noncovalently associated $\alpha\beta$ subunit heterodimers. Each subunit contains a large N-terminal extracellular domain, a transmembrane segment, and a cytoplasmic C-terminal tail. One unique aspect of integrin function is that the affinity for biological ligand can be up-regulated by a process termed inside-out signaling (1). This is particularly important during activation of leukocytes and platelets, where integrins are converted to high-affinity receptors in <1 s. It has been suggested that this rapid affinity up-regulation is accomplished by a conformational change in integrin extracellular domains triggered by cytoplasmic signaling pathways after cellular activation.

Several alternative models for conformational change have been proposed. Crystal structures obtained of the extracellular domain of αVβ3 in Ca^{2+} (2) or by subsequent soaking in Mn^{2+} and a cyclic Arg-Gly-Asp (RGD) peptide (3) revealed an unexpected bent conformation, in which the headpiece is folded over and makes extensive contacts with the tailpiece (Fig. 1*A*). Upon ligand binding, no change was seen at the interface between the I-like and hybrid domains, and only a slight rotation between the β-propeller and I-like domains and small movements within the I-like domain were seen. It was hypothesized that both the liganded and unliganded bent structures were in the active state (2, 3). In contrast, NMR, negative stain electron microscopy (EM) with image averaging, ligand binding, physicochemical, and mutational studies show that the bent conformation is physiologic and has low ligand-binding affinity and that activation results in a switchblade-like opening to an extended conformation (4, 5). Two extended conformers were seen that differed in whether there was an acute or obtuse angle between the I-like and hybrid domains, i.e., the closed (Fig. 1*B*) and open (Fig. 1*C*) conformations of the headpiece, respectively (5). The closed conformation of the headpiece resembles that seen in the αVβ3 crystal structure. Only the open conformation of the headpiece was seen when ligand was bound, suggesting that in the absence of crystal lattice contacts, ligand binding induced (*i*) a swing-out of the hybrid domain, and (*ii*) disruption of the headpiece–tailpiece interface in which the hybrid domain is prominent, leading to integrin extension (5). Lower resolution rotary shadowing EM studies from another group led to a completely different conclusion, that binding of cyclic RGD peptide results in separation of the α and β subunits in the headpiece and that separation between the α-subunit β-propeller domain and the β-subunit I-like domain induces the high-affinity state (6, 7). Based on the negative stain EM studies, we hypothesized that the opening of the angle between the I-like domain and the hybrid domain in β subunit is the key feature of the high-affinity conformer. To mimic this conformation, we have introduced a glycan wedge at the domain interface and have successfully engineered αIIbβ3, αVβ3, and α5β1 integrins that show constitutively high affinity. Furthermore, the results suggest that axial movement of the C-terminal helix of the β subunit I-like domain is responsible for affinity modulation, suggesting the existence of a common theme for activation of all integrins.

Materials and Methods

Plasmid Construction, Expression, and Ligand-Binding Activity of Integrins on Chinese Hamster Ovary (CHO)-K1 Cells. Plasmids coding for full-length human αIIb, β3, and β1 were subcloned into pcDNA3.1/Myc-His(+) or pEF1/V5-HisA, as described previously (5), and were introduced into the CHO-K1 cells by using calcium phosphate precipitation. After selecting the transfected cells in a medium containing 5 mg/ml geneticin G418 for 1 week, the surviving cells were assessed for integrin expression by flow cytometry using antibody AP3 to human β3 (American Type Culture Collection) or antibody TS2/16 to human β1 (8). The cells were then selected by fluorescence-activated cell sorting for expression of the desired level of αIIbβ3 or α5β1 integrins. Binding of fluorescein-labeled human fibrinogen and ligand mimetic antibody PAC-1 (gift from Sanford Shattil, The Scripps Research Institute, La Jolla, CA) was performed as previously described (5). For the binding of fibronectin fragment to human β1-expressing cells, the cells were incubated with 50 μg/ml biotinylated Fn_{9-10} (9) in the presence or absence of activating mAb TS2/16 (10 μg/ml) at room temperature for 30 min and stained with FITC-streptavidin (Zymed) followed by flow cytometry. Cell adhesion to human fibrinogen (Enzyme Research Laboratories, South Bend, IN) was determined by assaying cellular phosphatase (10).

Ligand-Induced Binding Site (LIBS) Expression. LIBS antibody AP5 was from the Fifth International Leukocyte Workshop (11), and LIBS-1, LIBS-6, and PMI-1 antibodies were obtained from Mark H. Ginsberg (The Scripps Research Institute). CHO-K1 cells

Abbreviations: EM, electron microscopy; LIBS, ligand-induced binding site; CHO, Chinese hamster ovary.

§To whom correspondence should be addressed. E-mail: takagi@cbr.med.harvard.edu.

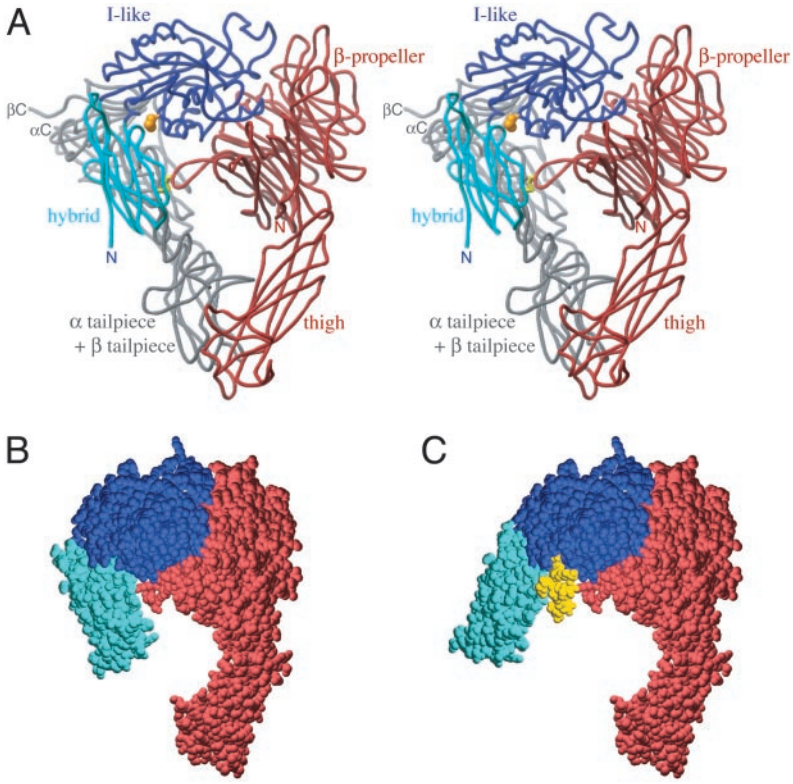

Fig. 1. The hybrid domain swing-out model of integrin activation. (*A*) Location of Asn-303 of β3 in the context of the bent conformation of the αVβ3 extracellular fragment. Stereo diagram of the crystal structure (2) is shown as a worm presentation. Note that the site of neoglycan introduction (Asn-303, gold CPK model) is located at the I-like domain/hybrid domain boundary and faces away from the tailpiece–headpiece interface. A mutationally introduced disulfide bridge between residue 307 in αV and 563 in β3 that locks the overall bent conformation is shown as a yellow bond. Headpiece segments are color-coded as follows: αV β-propeller and thigh domains in magenta; β3 I-like domain in blue; and β3 hybrid domain in cyan. Tailpiece segments (i.e., calf-1 and calf-2 domains of αV, I-EGF3, I-EGF4, and β-tail domains of β3) are shown in gray. The figure was prepared by RIBBONS (27). (*B*) The αVβ3 headpiece from the crystal structure. Each domain is color coded as in *A*. (*C*) Model of the high-affinity integrin headpiece. The hybrid domain of β3 (residues 55–107 and 352–434) was rotated $\approx$30° away from αV subunit about residue 106 and submitted to the SWISS-MODEL server for refinement (28). The $GlcNAc_2Man_7$ glycan chain (yellow) from human CD2 structure (1GYA) (29) was modeled into the inner side of the bend to simulate the glycan attachment at Asn-303. (*B* and *C*) CPK representations prepared with SWISSPDBVIEWER (30).

stably expressing wild-type or mutant αIIbβ3 were incubated with LIBS antibodies (10 μg/ml) at room temperature for 30 min, followed by staining with FITC-conjugated secondary antibody and flow cytometry.

Transient Transfection of 293T Cells. 293T cells were transiently transfected with wild-type or mutant integrin cDNAs by using calcium phosphate precipitation and were metabolically labeled with [^{35}S]cysteine/methionine as described (5). Labeled cell lysates were first immunoprecipitated with AP3 antibody, eluted with 0.5% SDS, and after the addition of 1% Nonidet P-40, were treated with or without 500 units of PNGase F (New England Biochemicals) at 37°C for 1 h. Material was subjected to nonreducing SDS/7% PAGE and fluorography.

Results

Design of Constitutively Active Mutant Integrin. To test the hypothesis that opening the interface between the hybrid and I-like domains regulates integrin affinity for ligand, we mutationally introduced an N-glycosylation site in the α5–β5 loop on the bottom of the I-like domain, where the angle with respect to the hybrid domain is most acute (Fig. 1*A*). This site is far from the ligand-binding site on the upper face of the I-like domain containing the metal ion-dependent adhesion site and thus should only enhance ligand binding allosterically. Furthermore, the site is distal from both the headpiece–tailpiece interface and the β-propeller-I-like domain interface (Fig. 1*A*) and thus should not directly affect either of these interfaces, which have also been suggested to regulate ligand binding. The β3 mutation Asn-305→Thr introduced the Asn-303–Ile-304–Thr-305 N-glycosylation sequon and is predicted to result in attachment of a bulky N-glycan wedge at Asn-303.

The N-Glycan Wedge Mutant Has High Affinity for Ligand. Wild-type or mutant β3 ($\beta3^{N305T}$) was cotransfected with wild-type αIIb subunit into CHO-K1 cells. Stable clones expressing similar levels of mutant and wild-type αIIbβ3 were selected. Similar binding to wild-type and mutant receptors by mAbs to multiple αIIb and β3 epitopes including AP3 (anti-β3), 7E3 (anti-β3), HA5 (anti-αIIb), and AP2 (anti-αIIbβ3 complex specific) (Fig. 2*A*) suggested that the mutant receptor adopts a native fold. Soluble ligand binding was measured by using two-color flow cytometry (5). Wild-type αIIbβ3 on CHO-K1 cells bound soluble fibrinogen and the ligand mimetic antibody PAC-1 only when stimulated by Mn^{2+} and activating mAb PT25–2 (Fig. 2 *B* and *C*). In contrast, αIIb$\beta3^{N305T}$ constitutively bound fibrinogen and PAC-1 antibody (Fig. 2 *B* and *C*). Binding by the mutant receptor in the presence of 5 mM Ca^{2+} was comparable with that of wild-type receptor maximally activated with Mn^{2+} and activating mAb and was not further increased by the addition of activating reagents. In contrast to the introduction of an N-glycosylation site, mutation of Asn-303 to Trp to introduce a bulky side chain (12) was not activating (data not shown), consistent with ample space for the Trp side chain in the closed interface.

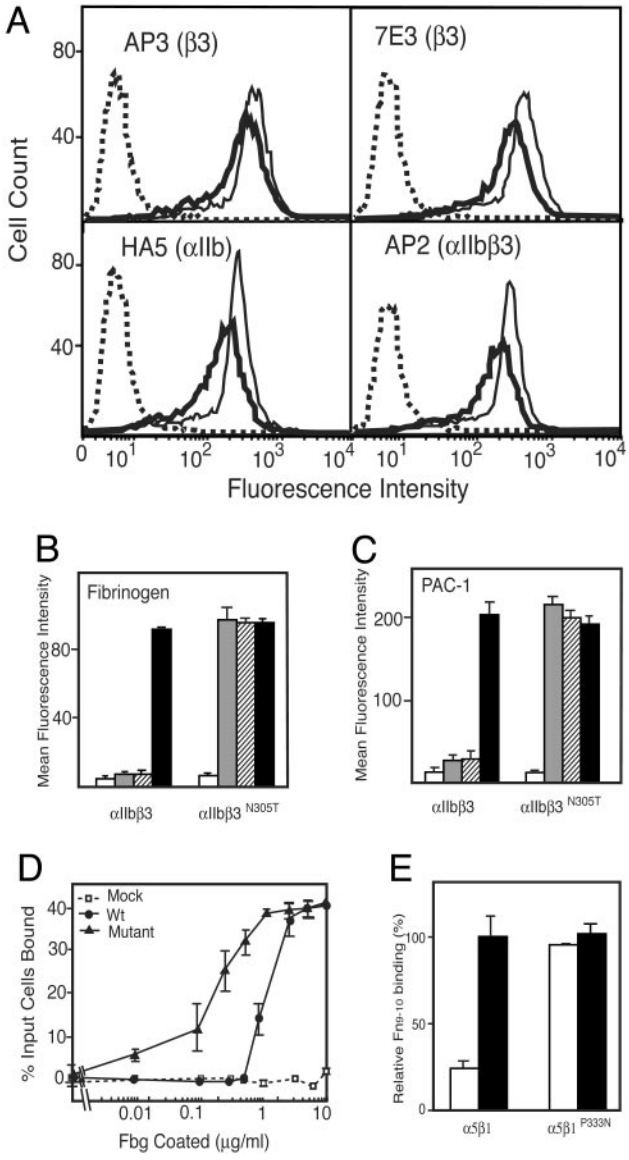

Fig. 2. Expression and ligand binding activity of glycan-wedge mutants. (*A*) Immunofluorescent staining of CHO-K1 transfectants. Cells express wild-type αIIbβ3 (thin line) or mutant αIIbβ3 (thick line) or are mock transfectants (dotted line). (*B* and *C*) Soluble ligand binding. Cells were incubated with FITC-fibrinogen (*B*) or PAC-1 (*C*) in the presence of 5 mM EDTA (white bar), 5 mM Ca^{2+} (gray bar), 1 mM Ca^{2+}/1 mM Mg^{2+} (hatched bar), or 1 mM Mn^{2+} plus 10 μg/ml PT25–2 mAb (black bar) at room temperature for 30 min. Binding was determined as described in *Materials and Methods* and was expressed as the mean fluorescence intensity. (*D*) Adhesion of wild-type αIIbβ3 (●), mutant αIIbβ3 (▲), or mock transfectants (□) to surfaces coated with fibrinogen at the indicated concentrations. Data are representative of three independent experiments, each in triplicate. (*E*) Binding of Fn_{9-10} fragment to cells expressing wild-type or mutant β1 integrin. Cells were incubated with 50 μg/ml biotinylated Fn_{9-10} in the presence (black bar) or absence (white bar) of 10 μg/ml anti-β1 activating mAb TS2/16 and probed with FITC-streptavidin. Relative amounts of ligand binding were normalized to a 100% value for binding to wild-type β1 cells treated with TS2/16, after subtraction of background binding obtained in the presence of 5 mM EDTA, and expressed as an average of two independent experiments.

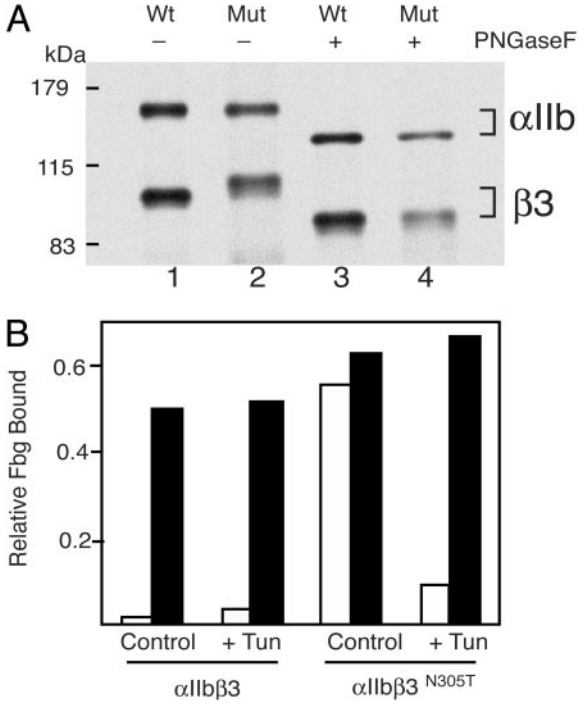

Fig. 3. Effect of N-glycosylation. (*A*) Immunoprecipitation. Lysates from ^{35}S-labeled 293T cell transfectants were immunoprecipitated with mouse anti-human β3 AP3. Precipitated wild-type (Wt) or mutant (Mut) material was treated with (+) or without (−) PNGase F for 1 h and subjected to nonreducing SDS/7.5% PAGE and fluorography. Positions of molecular size markers are shown on the left. (*B*) Effect of tunicamycin treatment on fibrinogen binding. Transiently transfected 293T cells were treated with (+Tun) or without (control) 1.5 μg/ml tunicamycin for 24 h before transfection and 48 h after transfection. FITC-fibrinogen binding was determined in the absence (white bar) or presence (black bar) of activating reagents. Binding was expressed as the percentage of mean fluorescence intensity relative to that of immunofluorescent staining with AP3 mAb to β3.

The affinity state of αIIbβ3^{N305T} was further tested in cell adhesion assays. Although high affinity is required for soluble ligand binding, basally active, i.e., low-affinity, αIIbβ3 can mediate cell adhesion to high-density substrates. Wild-type αIIbβ3 transfectants adhered to fibrinogen-coated surfaces at coating concentrations of $\geq$1 μg/ml (Fig. 2*D*). Parent CHO-K1 cells showed no adhesion even at the highest concentration of fibrinogen (Fig. 2*D*). In contrast, cells expressing αIIbβ3^{N305T} adhered to fibrinogen surfaces at coating concentrations as low as 10 ng/ml (Fig. 2*D*), demonstrating markedly augmented adhesiveness.

The Hyperactive Phenotype Is Due to the Introduced Glycan Chain. In 293T cell transient transfectants, the wedge mutant was hyperactive in soluble fibrinogen and PAC-1 binding assays just as in CHO-K1 cells (data not shown). Transiently transfected 293T cells were metabolically labeled, and αIIbβ3 complex was immunoprecipitated with β3 mAb AP3. Nonreducing SDS/PAGE showed that the αIIb subunits migrated similarly, whereas the mutant β3 migrated slower than wild-type β3, with an $\approx$3-kDa increase in molecular mass (Fig. 3*A*, lanes 1 and 2). Furthermore, this difference between wild-type and mutant β3 disappeared on deglycosylation by PNGase F (Fig. 3*A*, lanes 3 and 4). The increased molecular mass of the mutant β3 is therefore due to additional N-glycosylation, suggesting that the N305T mutation resulted in the attachment of a glycan chain at Asn-303.

To confirm the causative role of Asn-303 glycosylation of β3 in αIIbβ3 activation, transient transfectants were treated before and after transfection with the N-glycosylation inhibitor tunicamycin. Ligand binding by wild-type αIIbβ3 was unaffected by tunicamycin, as treated and untreated cells showed similar fibrinogen binding after stimulation with Mn and activating mAb (Fig. 3*B*). By contrast, tunicamycin treatment abolished the

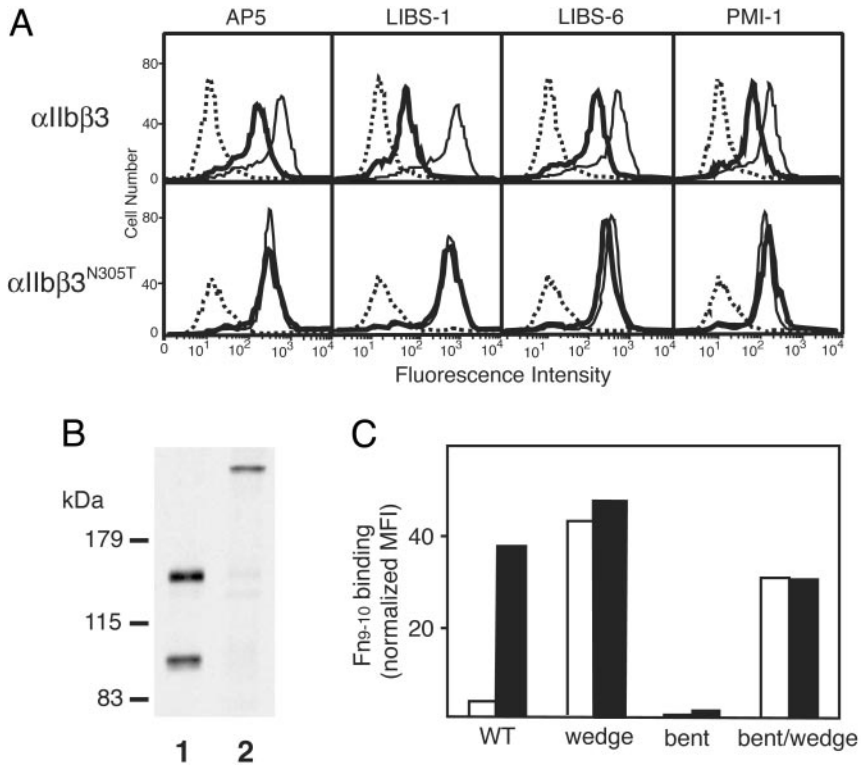

Fig. 4. Effect of glycan wedge on global unbending of β3 integrins. (*A*) Exposure of LIBS epitopes. Wild-type (*Upper*) or mutant (*Lower*) αIIbβ3 CHO cell transfectants were incubated with LIBS mAbs for 30 min at room temperature. Histograms represent binding in the presence of 5 mM Ca^{2+} (thick line) or 1 mM Mn^{2+} plus 100 μM GRGDSP peptide (thin line). Binding of control antibody is also shown (dotted histogram). (*B*) Wedge mutant of αVβ3 can be locked in a bent conformation. 293T cells were transiently transfected with wild-type or mutant αVβ3, metabolically labeled, and immunoprecipitated with AP3. Disulfide bond formation between Cys-307 of αV and Cys-563 of $\beta3^{N305T}$ is shown as a high-molecular-weight band in bent/wedge mutant (lane 2) after immunoprecipitation and nonreducing SDS/PAGE. Lane 1 shows wild-type αVβ3 as a control. (*C*) Activation of locked-bent αVβ3 by glycan-wedge mutation. Binding of biotinylated Fn_{9-10} to 293T cells transiently expressing various αVβ3 mutants in the presence (black bar) or absence (white bar) of activating mAb AP5 was determined. WT, wild type αV and β3; wedge, wild-type αV and $\beta3^{N305T}$; bent, αV^{G307C} and $\beta3^{S563C}$; bent/wedge, αV^{G307C} and $\beta3^{S563C/N305T}$. Fn_{9-10} binding is expressed as the percentage of mean fluorescence intensity relative to immunofluorescent staining with mAb AP3.

constitutive ligand-binding activity by αIIb$\beta3^{N305T}$, whereas like wild type it was still activatable by Mn and mAb (Fig. 3*B*). Therefore, carbohydrate attachment at residue β3–Asn-303 endowed the receptor with high affinity rather than the mutation of Asn-305 to Thr.

Activation of $\alpha5\beta1$ with a Glycan Wedge. To generalize these findings, similar mutations were designed in the integrin β1 subunit. The equivalent mutation in the α5–β5 loop, β1-Q312T, was not expressed well on the cell surface. Therefore, an N-linked site was introduced nearby in the α6–β6 loop with the β1-P333N mutation, which introduced the sequon Asn-333–Lys-334–Ser-335. This mutation was well expressed in stable CHO-K1 transfectants, in which human β1 associates with endogenous hamster α5 to make functional $\alpha5\beta1$ (13). Wild-type human β1 transfectants bound a biotinylated fibronectin fragment containing domains 9 and 10 (Fn_{9-10}) only when the integrin was activated with mAb TS2/16 to human β1 (Fig. 2*E*). By contrast, $\beta1^{P333N}$ transfectants bound Fn_{9-10} in the absence of mAb TS2/16 activation (Fig. 2*E*). Binding was mediated by transfected mutant human β1, as it was inhibited by anti-human β1 blocking mAb 13 (data not shown). Thus, a glycan wedge in the cleft between the I-like and hybrid domains can activate both β1 and β3 integrins.

The Glycan Wedge Favors the Extended Conformation of αIIbβ3. Activation and/or ligand binding change the conformation of αIIbβ3, resulting in the exposure of neo-epitopes called LIBS. Such epitopes are buried in the bent conformation in headpiece–tailpiece and α tail–β tail interfaces and are exposed in the extended conformation (4). To probe the conformational state of the mutant αIIbβ3, binding of a panel of LIBS antibodies was determined. The mAbs AP5 (anti-β3, residues 1–6), LIBS1 (anti-β3), LIBS6 (anti-β3, residues 602–690), and PMI-1 (anti-αIIb, residues 844–859) bound poorly to the cells stably expressing the wild-type αIIbβ3 in Ca^{2+} but bound maximally when incubated with Mn^{2+} and RGD peptide (14–16) (Fig. 4*A Upper*). In contrast, all LIBS mAbs stained cells expressing the glycan wedge mutant αIIbβ3 brightly even in Ca^{2+} in the absence of ligand, and no further increase was observed upon addition of Mn^{2+} and RGD peptide (Fig. 4*A Lower*). Another LIBS mAb D3 (anti-β3, residues 422–490) also bound constitutively to the mutant αIIbβ3 (data not shown).

Wedged Integrin Locked in a Bent Conformation Shows High Affinity. The hybrid domain is located in the headpiece and has a larger contribution than any other domain to the headpiece–tailpiece interface (5). The glycan wedge is predicted not to push the hybrid domain toward the tailpiece, but laterally out of the headpiece–tailpiece interface, and thus to indirectly destabilize it. Ligand-induced swing-out of the hybrid domain has been previously predicted to destabilize the bent conformation by the same mechanism, and the maximal exposure of LIBS epitopes in the wedge mutant accords with this model of integrin activation (5). The above studies did not define whether high ligand-binding affinity was a proximate effect of straightening the bend

between the I-like and hybrid domains or secondary to transition from the bent to extended integrin conformation. The $\alpha V\beta 3$ integrin can be locked in the bent conformation by introduction of an intersubunit disulfide bond between the α subunit β-propeller domain and β subunit I-EGF4 domain (Fig. 1*A*). The disulfide-locked integrin is inactive and resistant to activation by Mn^{2+} and antibodies unless a disulfide-reducing agent is added (5). The postulated lateral swing-out of the hybrid domain would not be blocked by this disulfide bond (Fig. 1*A*). Therefore, the two types of mutations were introduced into the same $\alpha V\beta 3$ integrin molecules. Immunoprecipitation and nonreducing SDS/PAGE confirmed complete formation of the disulfide bond between the αV head and $\beta 3$ tail, suggesting that the doubly mutant receptor was locked in the overall bent conformation (Fig. 4*B*, lane 2). This notion was further confirmed by the lack of binding by LIBS mAbs AP5, LIBS-1, LIBS-6, and D3 to $\alpha V^{G307C}\beta 3^{N305T/S563C}$, either in the presence or absence of RGD peptide (data not shown). Because we wanted to focus on conformational change within the ligand-binding site rather than on its accessibility, we used a small protein ligand, Fn_{9-10}, to minimize any influence of unbending on accessibility. The wedge mutation (N305T) constitutively activated the locked-bent receptor (i.e., $\alpha V^{G307C}\beta 3^{S563C}$) for binding to Fn_{9-10}, whereas locked-bent $\alpha V\beta 3$ without the wedge mutation remained incapable of ligand binding even after the addition of activating mAb (Fig. 4*C*). This result demonstrates that activation of high-affinity ligand binding by the wedge mutant is not secondary to adoption of the extended conformation of the integrin. When the larger ligand fibrinogen was used, however, the wedge-bent double mutant receptor did not show constitutively high activity (data not shown). This suggests that both the affinity of the ligand-binding site as well as its accessibility are important for binding of larger ligands.

Discussion

When liganded and unliganded receptors assume two distinct conformational states, it is generally possible to increase ligand affinity by stabilizing the liganded conformation because conformational change and ligand binding are thermodynamically linked (12, 17). Our findings support the proposal that the change in angle between the I-like and hybrid domains in the transition between the open and closed headpiece conformations regulates ligand-binding affinity (5). The findings do not support the proposal that the closed conformation of the headpiece is already in an active state and that no major interdomain conformational movements are associated with ligand binding (3). Our findings emphasize the importance of the angle between the β-subunit hybrid and I-like domains rather than separation between the α-subunit β-propeller and β-subunit I-like domains in integrin activation. Whereas our studies do not specifically address head separation, other results mitigate against it. The α and β subunits could not be distinguished from one another in EM studies that supported head separation (6), whereas higher resolution EM studies in which the α and β subunits could be distinguished showed no evidence for ligand-stimulated head separation (5), in agreement with many other EM studies (18–21). Furthermore, binding of cyclic RGD peptides stabilizes rather than destabilizes α and β subunit association (7, 22, 23), and binding of the Arg moiety of RGD to the α subunit and the Asp moiety to the β subunit across the intersubunit interface would be destabilized by head separation.

The β-subunit I-like domain has a similar fold to the I domain, which is present in a subset of integrin α subunits and serves as the major ligand-binding site in the integrins in which it is present. The I and I-like domains are each connected through both their N and C termini to the domains in which they are inserted, the α-subunit β-propeller and β-subunit hybrid domains, respectively. In the I domain, downward, axial displacement of the C-terminal α-helix causes rearrangement of residues that comprise the metal ion-dependent adhesion site, thereby increasing ligand affinity (24). The structural similarity between I and I-like domains suggests a similar regulatory mechanism, in which a downward movement of the C-terminal α-helix of the I-like domain would allosterically regulate the conformation of the metal ion-dependent adhesion site and increase affinity for ligands. Indeed, the glycan wedge-induced widening of the angle between the I-like and hybrid domains is predicted to be tightly linked to downward displacement of the C-terminal α-helix of the I-like domain, based on the overall topology of the interdomain connections (Fig. 5). Of the four secondary structural elements on either side of the two interdomain connections, three are internal β-sheet strands and hence are fixed in position by hydrogen bond networks. By contrast, the hydrogen bonds in an α-helix are all local, within the secondary structure element, and permit displacement relative to neighboring structural elements. Furthermore, the I-like domain α-helix connection to the hybrid domain β-sheet is the innermost connection, and a piston-like downward α-helix movement at this connection would result in swiveling about a fulcrum at the other connection, opening the interface to accommodate the nearby glycan wedge (Fig. 5).

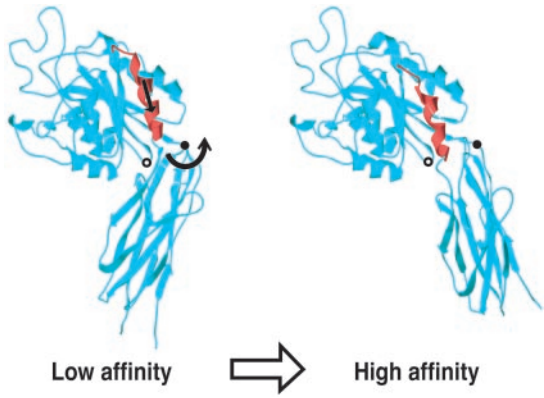

Fig. 5. Linkage between swing-out of the hybrid domain and pull-down of the I-like domain C-terminal helix. Model of $\beta 3$ head (I-like and hybrid domains) shows that outward swing of the hybrid domain about the pivot point (residue 106, filled circle) results in downward shift of the C-terminal helix of I-like domain (red). Position of Asn-303 used for glycan wedge mutation is denoted by an white circle.

Ligand mimetic cyclic RGD peptides can bind to the low-affinity, bent $\alpha V\beta 3$ receptor with the closed interdomain angle as shown by the crystal structure (3). Because the conformational and ligand-binding equilibria are linked, and the bent conformation is favored in the absence of cyclic RGD peptide binding, whereas the extended, open conformation is favored when cyclic RGD peptide is bound and crystal lattice restraints are absent (5), it follows that the affinity of cyclic RGD peptide is higher for the extended open than the bent conformation of $\alpha V\beta 3$. Ligand mimetics such as cyclic RGD peptides can be used at concentrations above their K_D for the low-affinity state of the receptor and therefore can be used to drive integrin conformational change according to the law of mass action. By contrast, physiological integrin ligands are generally encountered at concentrations below the K_D for the low-affinity state of the receptor; therefore, a change to a higher affinity conformation is usually required to drive ligand binding. Additionally, macromolecular ligands may lack access to the binding site in the bent integrin conformation. Physiologically, it is likely that integrins equilibrate between multiple conformational states rather than being locked in a specific conformation. Both signals within the cell that affect extracellular domain conformation and ligand

binding will affect these equilibria. In this regard, active regulation of integrins on the cell surface is best described as moving the equilibrium point within a conformational spectrum, rather than turning a switch on and off.

Receptor conformational change, especially rearrangements involving interdomain movements (12, 25, 26), is now gaining recognition as an important mechanism for controlling ligand binding. Thus, bulky amino acid side chain (12) and glycan wedges may have broad applications in designing mutant receptors with modified affinity. The present finding advances our knowledge of integrin activation at the molecular level. The successful application of the glycan wedge to β3 and β1 integrins implies that different integrins share the common principal of affinity modulation. The rational design of mutations that allosterically stabilize high-affinity or low-affinity conformations of integrins demonstrates marked advances in our understanding of the molecular basis of affinity regulation. This progress also holds out the promise that drugs might be designed that stabilize the low-affinity conformation of integrins, in contrast to the current generation of ligand-mimetic integrin antagonists that stabilize the high-affinity conformation.

We thank Drs. M. H. Ginsberg, M. Handa, L. Jennings, and S. Shattil for generously providing antibodies; B. S. Coller for critical reading of the manuscript; and Daniel P. DeBottis for technical assistance. This work was supported by National Institutes of Health Grant HL-48675.

1. Hynes, R. O. (2002) *Cell* **110,** 673–687.
2. Xiong, J.-P., Stehle, T., Diefenbach, B., Zhang, R., Dunker, R., Scott, D. L., Joachimiak, A., Goodman, S. L. & Arnaout, M. A. (2001) *Science* **294,** 339–345.
3. Xiong, J. P., Stehle, T., Zhang, R., Joachimiak, A., Frech, M., Goodman, S. L. & Arnaout, M. A. (2002) *Science* **295,** 151–155.
4. Beglova, N., Blacklow, S. C., Takagi, J. & Springer, T. A. (2002) *Nat. Struct. Biol.* **9,** 282–287.
5. Takagi, J., Petre, B. M., Walz, T. & Springer, T. A. (2002) *Cell* **110,** 599–611.
6. Hantgan, R. R., Paumi, C., Rocco, M. & Weisel, J. W. (1999) *Biochemistry* **38,** 14461–14474.
7. Hantgan, R. R., Rocco, M., Nagaswami, C. & Weisel, J. W. (2001) *Protein Sci.* **10,** 1614–1626.
8. Hemler, M. E., Sanchez-Madrid, F., Flotte, T. J., Krensky, A. M., Burakoff, S. J., Bhan, A. K., Springer, T. A. & Strominger, J. L. (1984) *J. Immunol.* **132,** 3011–3018.
9. Takagi, J., Erickson, H. P. & Springer, T. A. (2001) *Nat. Struct. Biol.* **8,** 412–416.
10. Tsuchida, J., Ueki, S., Saito, Y. & Takagi, J. (1997) *FEBS Lett.* **416,** 212–216.
11. Petruzzelli, L., Luk, J. & Springer, T. A. (1995) in *Leucocyte Typing V: White Cell Differentiation Antigens*, eds. Schlossman, S. F., Boumsell, L., Gilks, W., Harlan, J., Kishimoto, T., Morimoto, T., Ritz, J., Shaw, S., Silverstein, R., Springer, T., *et al.* (Oxford Univ. Press, New York), pp. 1581–1585.
12. Marvin, J. S. & Hellinga, H. W. (2001) *Nat. Struct. Biol.* **8,** 795–798.
13. Puzon-McLaughlin, W., Yednock, T. A. & Takada, Y. (1996) *J. Biol. Chem.* **271,** 16580–16585.
14. Frelinger, A. L., Cohen, I., Plow, E. F., Smith, M. A., Roberts, J., Lam, S. C. T. & Ginsberg, M. H. (1990) *J. Biol. Chem.* **265,** 6346–6352.
15. Frelinger, A. L., III, Du, X., Plow, E. F. & Ginsberg, M. H. (1991) *J. Biol. Chem.* **266,** 17106–17111.
16. Honda, S., Tomiyama, Y., Pelletier, A. J., Annis, D., Honda, Y., Orchekowski, R., Ruggeri, Z. & Kunicki, T. J. (1995) *J. Biol. Chem.* **270,** 11947–11954.
17. Mizoue, L. & Chazin, W. (2002) *Curr. Opin. Struct. Biol.* **12,** 459–463.
18. Weisel, J. W., Nagaswami, C., Vilaire, G. & Bennett, J. S. (1992) *J. Biol. Chem.* **267,** 16637–16643.
19. Erb, E. M., Tangemann, K., Bohrmann, B., Muller, B. & Engel, J. (1997) *Biochemistry* **36,** 7395–7402.
20. Du, X., Gu, M., Weisel, J. W., Nagaswami, C., Bennett, J. S., Bowditch, R. & Ginsberg, M. H. (1993) *J. Biol. Chem.* **268,** 23087–23092.
21. Hantgan, R. R., Lyles, D. S., Mallett, T. C., Rocco, M., Nagaswami, C. & Weisel, J. W. (2003) *J. Biol. Chem.* **278,** 3417–3426.
22. Thibault, G. (2000) *Mol. Pharmacol.* **58,** 1137–1145.
23. Billheimer, J. T., Dicker, I. B., Wynn, R., Bradley, J. D., Cromley, D. A., Godonis, H. E., Grimminger, L. C., He, B., Kieras, C. J., Pedicord, D. L., *et al.* (2002) *Blood* **99,** 1–7.
24. Shimaoka, M., Takagi, J. & Springer, T. A. (2002) *Annu. Rev. Biophys. Biomol. Struct.* **31,** 485–516.
25. He, X., Chow, D., Martick, M. M. & Garcia, C. K. (2001) *Science* **293,** 1657–1662.
26. Cho, H. S. & Leahy, D. J. (2002) *Science* **297,** 1330–1333.
27. Carson, M. (1997) *Methods Enzymol.* **277,** 493–505.
28. Peitsch, M. C. (1996) *Biochem. Soc. Trans.* **24,** 274–279.
29. Wyss, D. F., Choi, J. S., Li, J., Knoppers, M. H., Willis, K. J., Arulanandam, A. R. N., Smolyar, A., Reinherz, E. L. & Wagner, G. (1995) *Science* **269,** 1273–1278.
30. Guex, N. & Peitsch, M. C. (1997) *Electrophoresis* **18,** 2714–2723.